International Journal on Magnetic Particle Imaging
Vol 12, No 1, Suppl 1, Article ID 2603013, 3 Pages

Proceedings Article

Reduced-Order Modeling of Nanoparticle Magnetization Dynamics

Sevil Dilge Gulsun [a,b*] · Asli Alpman [a,b,c] · Emine Ulku Saritas [a,b]

[a] Department of Electrical and Electronics Engineering, Bilkent University, Ankara, Turkey
[b] National Magnetic Resonance Research Center (UMRAM), Bilkent University, Ankara, Turkey
[c] Department of Electrical Engineering and Computer Sciences, University of California Berkeley, CA, USA
*Corresponding author, email: dilge.gulsun@bilkent.edu.tr

Abstract

The coupled Brown-Néel rotation model formulates the nanoparticle magnetization dynamics as a system of ordinary differential equations that are computationally demanding to solve. In this work, we propose utilizing a proper orthogonal decomposition approach for reduced-order modeling of magnetization dynamics, providing significant computational speedup while preserving accuracy.

I. Introduction

Modeling the magnetization dynamics for magnetic nanoparticles (MNP) helps understand their magnetic particle imaging (MPI) signal under varying conditions. For this purpose, the coupled Brown–Néel rotation model, which originates from the stochastic Fokker-Planck Equations (FPE) for MNP magnetization, was previously presented as a system of coupled ordinary differential equations (ODEs) [1]. We previously showed that this model can be used for signal prediction via a model-based dictionary approach [2]. However, solving the coupled ODE is computationally demanding. Recent work has proposed computational speedup by utilizing Fourier neural operators, however, the training process still requires solving the ODE for a wide range of MNP parameters [3, 4].

In this work, we propose utilizing a proper orthogonal decomposition (POD) approach that derives a reduced order model (ROM) of the magnetization dynamics to provide computational acceleration while maintaining high accuracy.

II. Theory

Full-order model (FOM) for the coupled ODE can be expressed as $\dot{\mathbf{y}}(t) = \mathbf{F}(t)\mathbf{y}(t)$, where $\mathbf{y}(t) \in \mathbb{R}^N$ and N relates to the truncation level of spherical harmonics expansion [1]. In addition, $\mathbf{F}(t) \in \mathbb{R}^{N\times N}$ depends on the applied field at time t and MNP parameters, but not on $\mathbf{y}(t)$. FOM can be numerically solved to compute the snapshot matrix $\mathbf{Y} = [\mathbf{y}_1\ \mathbf{y}_2\ \cdots\ \mathbf{y}_M] \in \mathbb{R}^{N\times M}$, where M is the number of time samples and $\mathbf{y}_k \in \mathbb{R}^N$ is the state vector at time point k.

POD is a model order reduction technique that approximates complex systems in a lower dimensional subspace [5]. Given $\mathbf{Y}$, POD aims to find a set of orthonormal basis vectors $\{\boldsymbol{\phi}_i\}_{i=1}^r,\quad \boldsymbol{\phi}_i \in \mathbb{R}^N$ such that their span best approximates the state vectors in the least-squares sense:

$$\min_{\{\boldsymbol{\phi}_i\}_{i=1}^r} \sum_{k=1}^{M} \left\| \mathbf{y}_k - \sum_{i=1}^{r} (\boldsymbol{\phi}_i^\top \mathbf{y}_k)\boldsymbol{\phi}_i \right\|_2^2 \tag{1}$$

The POD basis is given by the most dominant r left singular vectors of $\mathbf{Y}$. From the low-rank singular value decomposition (SVD) approximation, $\mathbf{Y} \approx \mathbf{U}_r\boldsymbol{\Sigma}_r\mathbf{V}_r^\top$, where $\mathbf{V}_r \in \mathbb{R}^{M\times r}$ contains the right singular vectors, $\boldsymbol{\Sigma}_r \in \mathbb{R}^{r\times r}$ is a di-

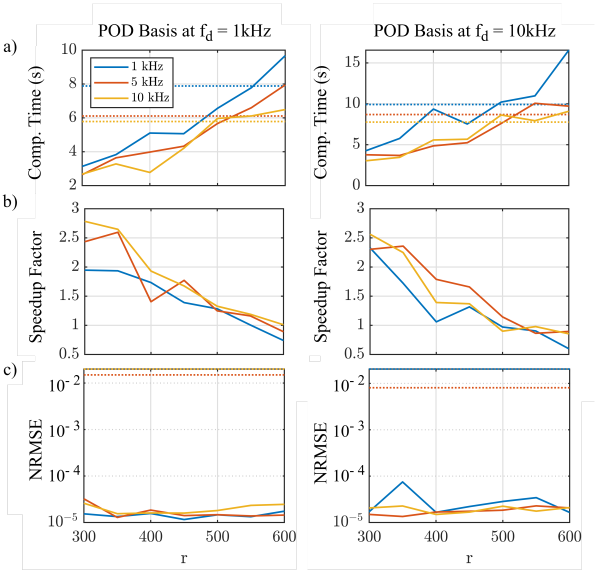

Figure 1: Performance of the POD basis across different DF frequencies. (a) Computation time, (b) speedup factor, and (c) NRMSE when the DF frequency is changed after computing the POD basis at [Left] $f_d = 1\,\text{kHz}$ and [Right] $f_d = 10\,\text{kHz}$. For each case, the computed basis is utilized at three different DF frequencies (see legend). Dashed lines indicate (a) the computation time for FOM and (c) the baseline NRMSE between the FOM solutions at different settings. NRMSE was computed with the FOM solution at each setting taken as ground truth. Other parameters were $d_c = 20\,\text{nm}$, $K = 6\,\text{kJ/m}^3$, $B_d = 15\,\text{mT}$.

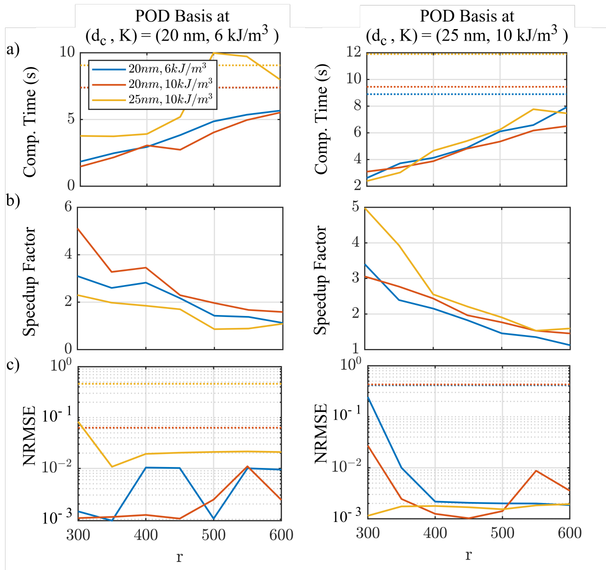

Figure 2: Performance of the POD basis across different MNP parameters. (a) Computation time, (b) speedup factor, and (c) NRMSE when the MNP parameters are changed after computing the POD basis at [Left] $(d_c, K) = (20\,\text{nm}, 6\,\text{kJ/m}^3)$ and [Right] $(d_c, K) = (25\,\text{nm}, 10\,\text{kJ/m}^3)$. For each case, the computed basis is reused to reconstruct the magnetization response at three different sets of MNP parameters (see legend). NRMSE was computed with the FOM solution at each setting taken as ground truth. Other parameters were B_d =15 mT, f_d=5 kHz.

agonal matrix of singular values, and $\mathbf{U}_r = [\boldsymbol{\phi}_1, \ldots, \boldsymbol{\phi}_r] \in \mathbb{R}^{N\times r}$ forms the POD basis matrix. The solution can be represented in the POD subspace as $\hat{\mathbf{y}}(t) = \mathbf{U}_r\,\mathbf{a}(t)$, where $\mathbf{a}(t) \in \mathbb{R}^r$ are the unknown basis coefficients. Then, the ROM for the coupled ODE becomes $\dot{\mathbf{a}}(t) = \tilde{\mathbf{F}}(t)\mathbf{a}(t)$, where $\tilde{\mathbf{F}}(t) = \mathbf{U}_r^\top\,\mathbf{F}(t)\mathbf{U}_r \in \mathbb{R}^{r\times r}$. With $r < N$, the matrix size of the ODE system becomes significantly smaller, speeding up the computation time.

III. Materials and Methods

The proposed POD approach was evaluated on different drive field (DF) frequencies and MNP properties. The DF amplitude was fixed at $B_d = 15\,\text{mT}$, while three different DF frequencies of $f_d = 1\,\text{kHz}, 5\,\text{kHz}, 10\,\text{kHz}$ were utilized. In addition, three different MNPs with the following core diameters (d_c) and anisotropy constants (K) were utilized: $(d_c, K) = (20\,\text{nm}, 6\,\text{kJ/m}^3)$, $(20\,\text{nm}, 10\,\text{kJ/m}^3)$, $(25\,\text{nm}, 10\,\text{kJ/m}^3)$.

First, we constructed $\mathbf{F}(t)$ and solved the FOM for a selected parameter configuration, and then computed the basis matrix $\mathbf{U}_r$. Then, at a different parameter configuration, we constructed $\mathbf{F}(t)$, computed $\tilde{\mathbf{F}}(t)$ using the basis matrix, solved the ROM, and reconstructed $\hat{\mathbf{y}}$. ODEs were solved using *ode15s* built-in function of MATLAB, with N=900 for FOM and $r < N$ for ROM.

IV. Results and Discussion

Figure 1 shows the robustness of the POD basis across different DF frequencies. For each column, the POD basis generated at a selected DF frequency is used for solving the ROM at a different DF frequency. In Figure 1, the normalized root mean square error (NRMSE) is below 10^{-4} in all cases, with the computation time substantially reduced for lower r. Likewise, the speedup factor, defined as the ratio of the FOM and ROM computation times, increases for smaller r, demonstrating the computational advantage of the proposed approach.

Figure 2 demonstrates how well a POD basis can represent systems with different MNP parameters. In this case, the NRMSE remains below 10^{-1} for larger r. Note that the NRMSE values in Figure 2 are larger than those in Figure 1, implying that the MNP parameters have a bigger impact on the magnetization response when compared to the DF frequency. In addition, Figure 2 shows that the POD basis computed for a larger core diameter yields generally lower and more stable NRMSE trends, implying that it can more successfully capture the response at different MNP characteristics. Figure 3 illustrates this observation by comparing the ROM and FOM solutions for $(d_c, K) = (20\,\text{nm}, 6\,\text{kJ/m}^3)$. Here, the ROM solution uses the POD basis computed for a larger core diameter of $d_c = 25\,\text{nm}$ to successfully reconstruct the magnetization

10.18416/ijmpi.2026.2603013

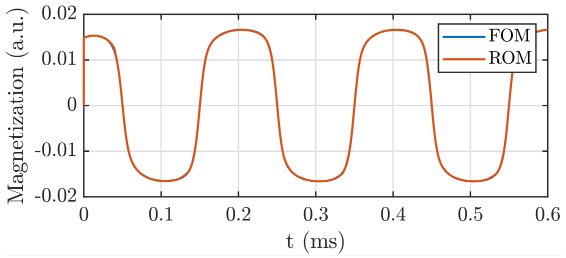

Figure 3: Comparing ROM and FOM solutions for $(d_c, K) = (20\,\mathrm{nm}, 6\,\mathrm{kJ/m^3})$, as an example case from Figure 2. Here, ROM uses the POD basis constructed for $(d_c, K) = (25\,\mathrm{nm}, 10\,\mathrm{kJ/m^3})$, with $r = 600$. With the FOM solution taken as the ground truth, NMRSE $= 1.86 \times 10^{-3}$ for ROM. Other parameters were $B_d = 15\,\mathrm{mT}$, $f_d = 5\,\mathrm{kHz}$.

response at different MNP parameters.

For the cases considered in this work, the singular values decayed rapidly, with the dominant singular values concentrating within approximately the first $r=100$ modes. However, for $r < 300$, the ODE solver failed to satisfy the prescribed tolerances, indicating numerical instability for small r. Hence, the values of r utilized in this work were chosen to balance the theoretical benefits of the low-rank approximation with the practical limitations of the ODE solver.

In this work, because the FOM for the coupled ODE system was solved only for 1D DFs, the proposed approach was also evaluated in this setting. While the extension to higher dimensional DFs remains a future work, the proposed approach can potentially yield even greater benefits in those more computationally demanding settings.

V. Conclusion

In this work, we demonstrated that POD enables efficient reduced-order modeling of MNP magnetization dynamics, with significant computational speed-up and high generalization performance.

Acknowledgments

This work was supported by TUBITAK grants 22AG016/23AG005 and 122E162. This publication is based upon work from COST Action CA23132 NexMPI, supported by COST (European Cooperation in Science and Technology).

Author's statement

Conflict of interest: Authors state no conflict of interest.

References

[1] J. Weizenecker. The fokker–planck equation for coupled brown–néel-rotation. *Physics in Medicine & Biology*, 63(3):035004, 2018, doi:10.1088/1361-6560/aaa186.

[2] A. Alpman, M. Utkur, and E. U. Saritas. Mnp characterization and signal prediction using a model-based dictionary. *International Journal on Magnetic Particle Imaging*, 8(1), 2022, doi:10.18416/ijmpi.2022.2203017.

[3] T. Knopp, H. Albers, M. Grosser, M. Möddel, and T. Kluth. Exploiting the fourier neural operator for faster magnetization model evaluations based on the fokker–planck equation. *International Journal on Magnetic Particle Imaging*, 9(1), 2023, doi:10.18416/IJMPI.2023.2303003.

[4] M. H. Kayapinar, A. Alpman, and E. U. Saritas. Fourier neural operator for coupled brown–neel rotation model. *International Journal on Magnetic Particle Imaging*, 10(1), 2024, doi:10.18416/ijmpi.2024.2403008.

[5] K. Kunisch and S. Volkwein. Galerkin proper orthogonal decomposition methods for a general equation in fluid dynamics. *SIAM Journal on Numerical Analysis*, 40(2):492–515, 2003.

